MACHINE-LEARNING FOR AUTOMATED FIBER PLACEMENT FOR MANUFACTURING EFFICIENCY AND PROCESS OPTIMIZATION

Waruna Seneviratne, John Tomblin and Upul Palliyaguru
National Institute for Aviation Research (NIAR), Wichita State University (WSU)
1845 Fairmount Street, Wichita, Kansas, 67260, USA

ABSTRACT

In order to meet aggressive demand, aircraft manufacturing processes must undergo significant technology advancements and future manufacturing engineers must be equipped with advanced hybrid, scalable, flexible, and extensible tools to adapt to growing complexities. Global aircraft manufacturers are aggressively seeking methods for advancing manufacturing technologies through automation and innovative materials/processes that increase manufacturing rates and efficiency. With the advancement of sensor technologies and manipulators, industrial robots are now capable of performing non-routine complex functions such as labor-intensive advanced composite layup that typically require meticulous, trained technicians. Automated fiber placement (AFP) has the potential to significantly decrease lead-time with increased material yield and production rates due to fewer interruptions and improved consistency. With the use of advanced sensors, process simulation software, and in-process inspection systems, labor-intensive nondestructive inspection for quality assurance can be automated for minimizing interruptions and to significantly improve part quality. In-process inspection systems equipped with advanced sensors is deployed for automatically identifying manufacturing defects and feed digital information into machine learning algorithms to take corrective actions on subsequent manufacturing runs to improve part quality. This approach, which develops a digital manufacturing twin for supporting sustainment activities, also fits well into the Factory of the Future concept and will aid in increasing production rates of commercial and defense aircraft.

Keywords: Automated fiber placement, in-process inspection, machine learning; small training datasets; training data model development

Corresponding author: Waruna Seneviratne (waruna@niar.wichita.edu)

1. INTRODUCTION

Worldwide demand for general, commercial and military aircrafts increase rapidly. Over the next few years, the annual net growth of active global commercial fleet will see a 3.3 % growth increasing the fleet size to approximately 37,978 from the current 26,307 fleet size. The growth in fleet is forecast to peak at 4.2 % annually over the next five years and then decrease to 3.3 percent in the second five years as the rate of deliveries decreases [1]. In order to fulfill the growing demand, significant changes are required in the manufacturing methodology, leading to the current focus on state of the art manufacturing technologies and innovative materials and processes.

Advanced manufacturing technologies such as automated fiber placement (AFP) and automated tape laying (ATL) are currently being used in aircraft production minimizing the technician involvement. Along with the automated manufacturing techniques, advanced thermoset and thermoplastic composite material systems are currently under development and evaluation to manufacture high quality aircraft parts at a higher throughput. However, the current automation manufacturing technologies rely on manual or time-intensive inspection techniques to ensure the engineering requirements of the structure being built. In most applications, these are technician heavy methodologies affecting the up time of the AFP robots performing the fabrication tasks. Current industry practice is to perform 100 percent manual inspections, in most cases basic visual inspections. The downtime of the manufacturing AFP system varies from 30-70% of their effective times based on how complex the inspection routes are. Considering the laminated nature of the advanced composites materials, repetitive inspection are conducted on each layer, further increasing the inspection time thus, affecting the efficiency and the throughput of the manufacturing process.

In support of decreasing the downtime of the AFP system due to manual inspections, automated in-process inspection methodologies can be used. Advances in the sensor technologies provide a wide variety of techniques that can be utilized for in-process inspection tasks. Specific sensor types can be utilized for effectively detecting certain manufacturing defects or features. With advanced sensors, information about the structure can be captured during manufacturing. Based on the sensor type utilized in in-process inspection activities, changes in the out of plane dimensional integrity, color gradient and thermal response can be correlated to a defect type or an anomaly. With the advances in the sensor technologies (higher resolution and data acquisition frequency) utilized in capturing dimensional measurements, optical color gradients and thermal response of the structure during the fabrication process, a large amount of data is generated for analysis in the defect to sensor data correlation activities. The correlation efforts to accurately categorize the damage type become the bottleneck in the inspection process. This falls into the category of big data analysis.

Machine learning (ML) can be utilized in support of analyzing the inspection data in the correlation efforts to categorize the defect type. Machine learning is a proven methodology in object classification and detection with a high probability of detection (POD) and accuracy. The key factors in an accurate ML model are the architecture and training dataset. There are many ML models available in the current open-source literature that provide a classification and detection accuracy of upwards of 90%. The POD and accuracy of detection solely depend on the quality and exemplariness of the training dataset. Key challenge of acquiring a reliable data source from actual defects in the production limits the accuracy of the ML model. Development of AFP defect models and numerically varying the parameters associated with each defect type to generate training datasets are investigated in this research. Geometrical models for three selected AFP defect types are developed varying the defect parameters, training data size and dataset type. Table 1 illustrates the varying parameters used for ML model training. Models developed with training dataset are based on existing datasets that are validated for classification accuracy.

Table 1. Summary of defect parameters and training dataset

Defect Type	Training Dataset Type	Num. of Training Images	Pixel Size of the Training Image	Validation Data Type	Validation Images per Defect
Gap Missing Tow Overlap	GM - No Noise GM - Simulated Noise PD	32 1024 10K	1 X Defect Length 3 X Defect Length 1 X 1600 3 X 1600 3 X 1600 (DA)	SD - No Noise SD - Simulated Noise PD	2000 1200

GM - Geometrical Model; PD - Profilometer Data; DA - Defect Annotated; SD - Simulated Defect

2. EXPERIMENTAL APPROACH

A laser profilometer manufactured by Keyence was used for the geometrical inspections to validate the ML classification accuracy. The profilometer was mounted to a XY gantry system. 0.5-inch tows were placed on a flat aluminum tool using an Electroimpact (EI) AFP machine for inspections. Multiple training datasets were generated to train the ML model. Trained model was validated with multiple datasets for classification accuracy.

2.1 Hardware and Experimental Setup

2.1.1 The Keyence Laser Profilometer

Keyence LJ V-7080 laser profilometer was used to capture the out-of-plane geometrical changes in the fiber tows against a flat tool. The LJ7080 profilometer was connected to a LJV7000 for processing the data (Figure 1). The profilometer has a working distance range of 57 to 103 mm. Based on the working distance, it captures data in a line ranging from 25-39 mm, recording 800 data points along the measurement line. The non-contact profilometer was placed on an inspection gantry and the surface under investigation was kept at a distance of approximately 100 mm to maximize the measurement line length. The LJ700 encoder is capable of incorporating two V7080 laser profilometer. For the inspections performed for tasks outlined in this research, two profilometers were used to obtain a total measurement line length of approximately 80 mm. With the two profilometers, a total of 1600 points were acquired in an 80mm inspection length providing a point resolution of 0.05 mm. Data from the encoder was transmitted to the data acquisition workstation using a high-speed wireless fidelity (Wi-Fi) network. An average data acquisition frequency of 40 Hz was used.

(a)Keyence LJ-V7080 profilometer and LJ7000IP decoder

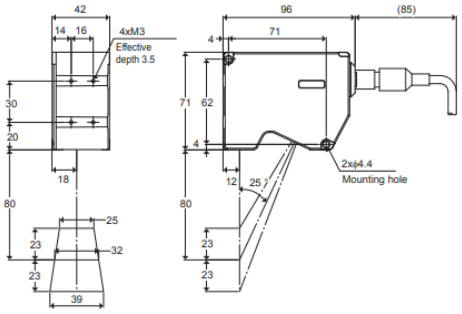

(b) Keyence LJ7080 Profilometer working envelope

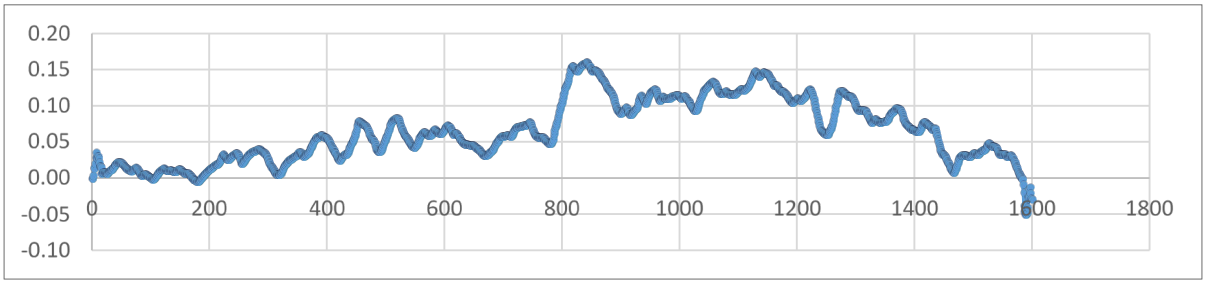

(c) Sample data from Keyence LJ7080 profilometer

Figure 1. Keyenece profilometer information.

2.2 Training Dataset Development and Manufacturing of Experimental Defects

EI AFP robot with ½" 8-tow configuration was used to layup five courses of Toray T1100GC-24K/3960 unidirectional tape material on a flat aluminum tool. The overall width of each course was 4-inches. One of the courses was used to manually induced AFP defect types to support this investigation. The gap defects were created by carefully cutting off a section of the tow. For the missing tow defect formation, an entire tow was removed from a course section. The overlap defects were created by placing the removed tow overlapping one of the adjacent tows. Manufactured defects were inspected with the profilometer and an optical camera. Figure 2 illustrates the optical and profilometer inspections performed on the fabricated defects.

AFP defect types discussed above were investigated under the microscope to understand the formation of the defects and their physical geometry. Based on the information, simplistic geometrical models were developed for gaps, missing tows, and overlaps. The defects were segmented into various sections based on their physical appearance. Figure 3 illustrates the critical sections in the gap/missing tow and overlap defects. The variation between the gap and missing tow was simulated by increasing the c-section length shown in Figure 3.

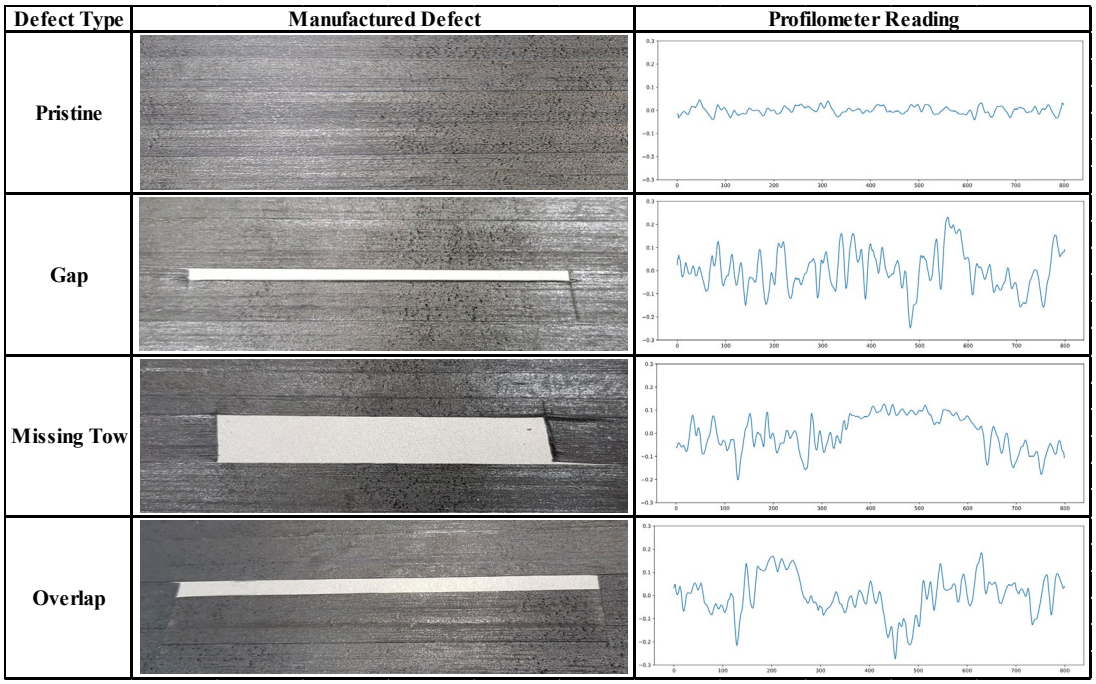

Figure 2. AFP defects under investigation with optical and geometrical inspections.

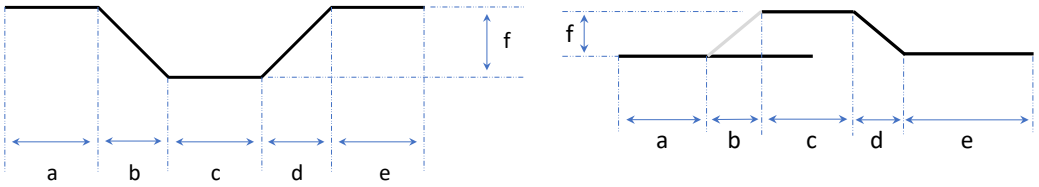

(a) Geometrical model of gap/missing tow defect configuration

(b) Geometrical model of overlap defect configuration

Figure 3. Geometrical models for AFP defect configurations.

The variables outlined in each defect type may subject to change based on the AFP fabrication parameters such as heat, speed and compaction force. These parameters are associated with the fabrication process specification followed during the manufacturing process. An algorithm was developed using C#.NET and Python programming languages to automate the creation of the defects. The parameters a through f (Figure 4) were input into the software along with the number of repetitions required. Additionally, the point gaps (point resolution of the profilometer) was specified to the software for training image generation process. Figure 4 illustrates the training dataset generator based on geometrical models for gap defects. The generated defect data were converted into gray scale images and used in the training of the ML models.

During the training dataset development, the height of the images generated was kept constant at one and three pixels. The length of the defects was varied to be the total length of parameters a through e. The second configuration used for the length of the training data set was kept constant at 1600 pixels with defect being added at a random location of the line. This was performed to simulate the geometrical inspection data format output by the profilometer.

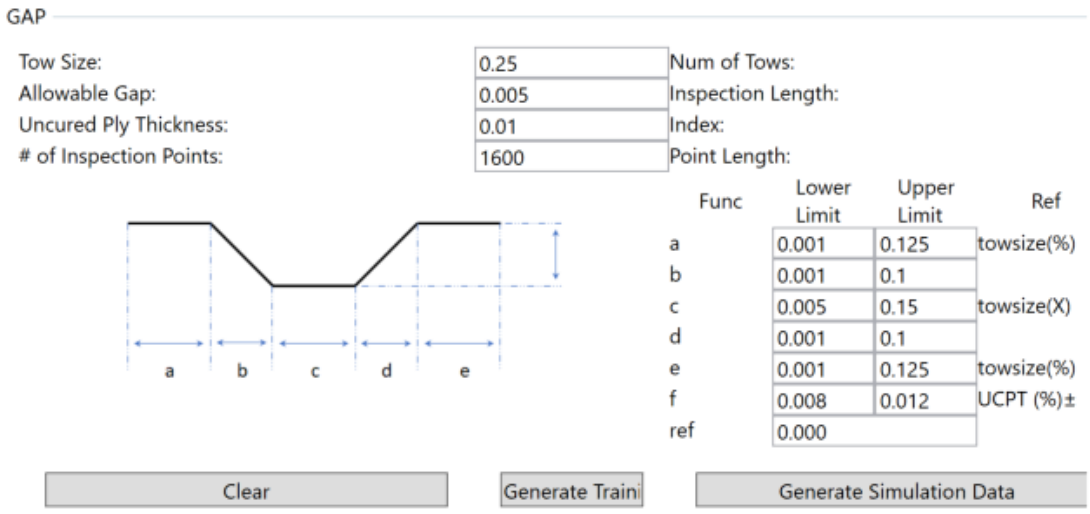

Figure 4. C#.NET interface of the training dataset generator for gap defects.

Similar approach was used to develop validation data, the length of the total geometrical data was kept constant at 1600 pixels for all validation datasets while placing the defect generated per the geometrical model in a random location along the 1600 pixel line.

2.2.1 Geometrical Model – No Noise (GMNN)

The GMNN was created based on the simplified representation of a defect, with no surface roughness or variation presented in the profilometer scan. They were generated through an algorithm that used lower and upper size limits for each section of a defect based on the geometrical models. The depth variation was specified to the algorithm based on a fixed tolerance. Both training and testing profiles are condensed and converted to grayscale images of 3 pixels of height and a user input number of pixels for length in the ML model. An example of each validation defect as well as the generated line image is presented in Figure 5.

Defect	Simulated Gray Scale Image	Simulated Profilometer Line
Pristine		
Gap	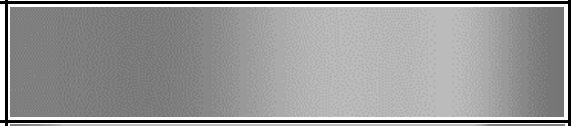	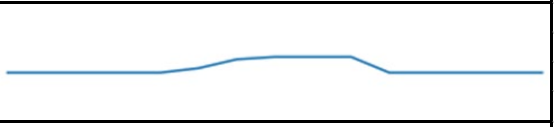
Missing Tow		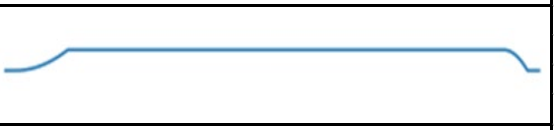
Overlap	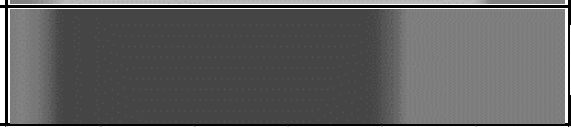	

Figure 5. Sample training images generated from GMNN.

2.2.2 Geometrical Model – Simulated Noise (GMSN)

The GMSN training datasets were generated following a similar algorithm as GMNN datasets. However, a random noise generator function was used in all the data to simulate the surface roughness, instrumental noise and data acquisition errors. The noise was generated by following a Gaussian distribution with a given mean of 0.0, and standard deviation of 0.0015, in order to generate random values to be added to the idealized defect data. The defects created with this parameter and their corresponding generated images are shown in Figure 6.

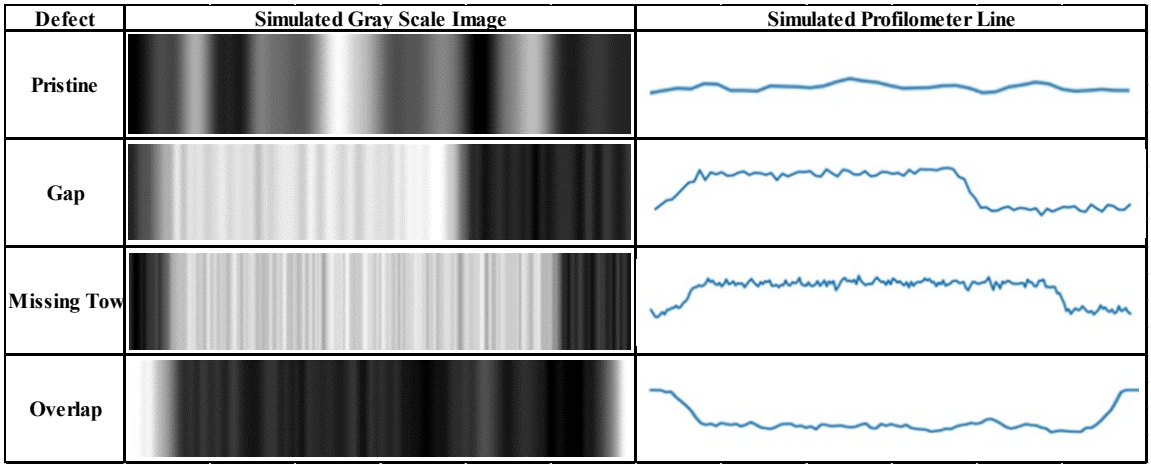

Figure 6. Sample training images generated from GMSN.

2.2.3 Profilometer Dataset (PD)

During development of the profilometer datasets, three profilometer datasets (one for each defect type) were analyzed and the values were separated into sections b, c and d as seen in Figure 3. New defect section lengths were generated by querying points at different intervals from the original curves. The height f was assigned by selecting a value within an upper and lower boundary chosen from observing real profilometer dataset readings. This resulted in new profilometer training datasets constructed from real sensor information, yielding the highest-fidelity generated set for training out of all datasets. Figure 7 illustrates different types of defects training data created using PD.

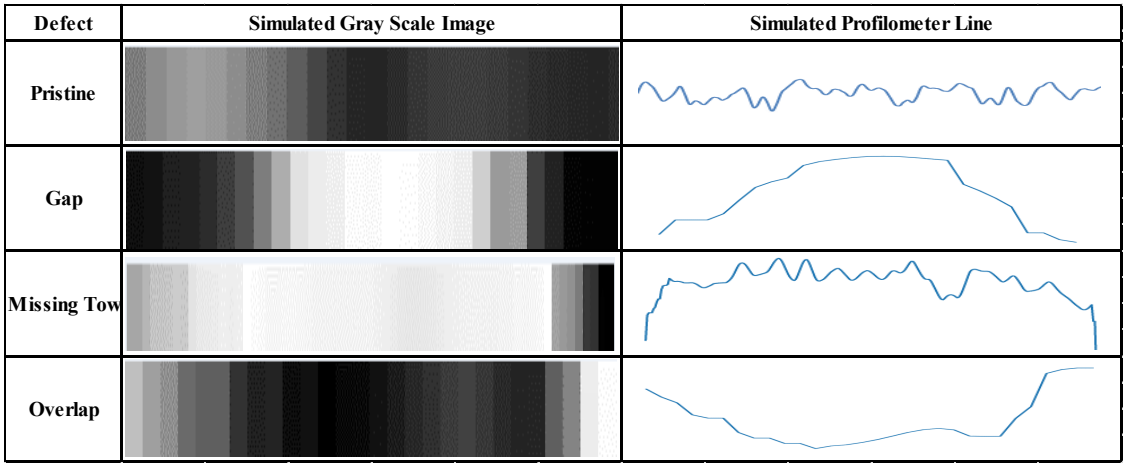

Figure 7. Sample training images generated from PD.

2.3 Machine Learning Models

Object detection (OD) ML models were used to classify and detect various AFP defects types. Tensorflow OD application programming interface (API) 2.0 was used in the ML developmental work for the research. The existing ML models from the API were used as the model architecture. The models were primarily used to detect trained objects. The pre-trained models were trained with a variety of datasets generated to evaluate the classification and detection accuracy. The objective of this evaluation was to assess the efficiency of the training data developed using the geometrical models.

2.3.1 Machine Learning Model Architecture

The ML model architecture used for defect detection model was single shot-multibox detector, (SSD) resnet 50. The head component used in the model architecture is illustrated in Figure 8. SSD head model architecture is illustrated in Figure 9.

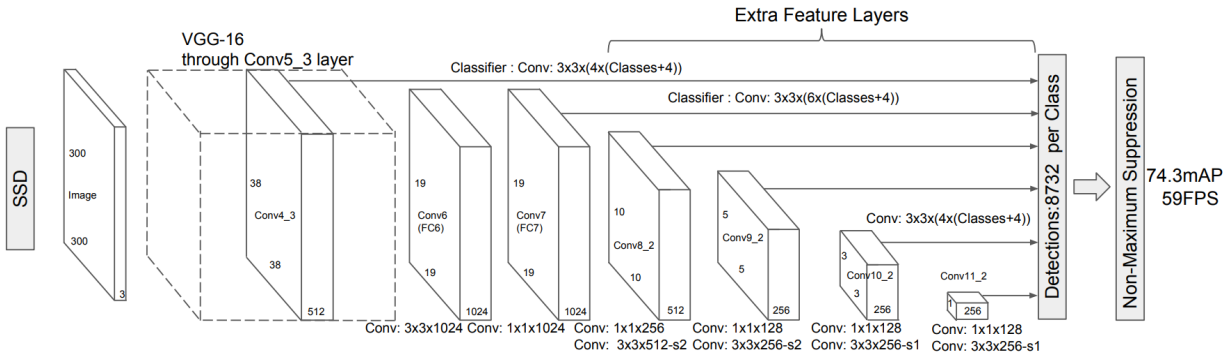

Figure 8. SSD Head model architecture [2]

The SSD resnet 50 model architecture was chosen as the pilot ML model for AFP defect detection tasks, due to the introduction of deep residual learning framework, allowing for resnet 50 to escape the issue of shallow networks. Deep residual networks consist of convolution, pooling, activation, and fully connected layers that are connected to similar layers one after the other as demonstrated in Figure 9. Between each of these individual combinations is an Identity Connection, allowing for past information to be passed to other layers down the network, and Residual Mapping, allowing for error values from the previous layer to be passed to the input of the next layer. The use of the identity mapping is that it allows for an additional pathway for gradients to be passed to other residual blocks in the network. The multiple connections between past and present residual blocks allow for resnet 50 to achieve greater accuracy while also allowing for deeper architectures in convolutional models. Additionally, SSD Resnet 50 was used for the classification of AFP defects. To increase the detection efficiency, SSD divides and defect images into multiple cell. Anchor boxes were pre-defined based on the defect types, and each one was compared with the bounding box detected until the anchor box with the highest degree of overlap was found.

The objective of selecting a single ML model architecture for validation of multiple model training dataset was to evaluate the effectiveness of utilizing generated training datasets on the accuracy of the classification and detection.

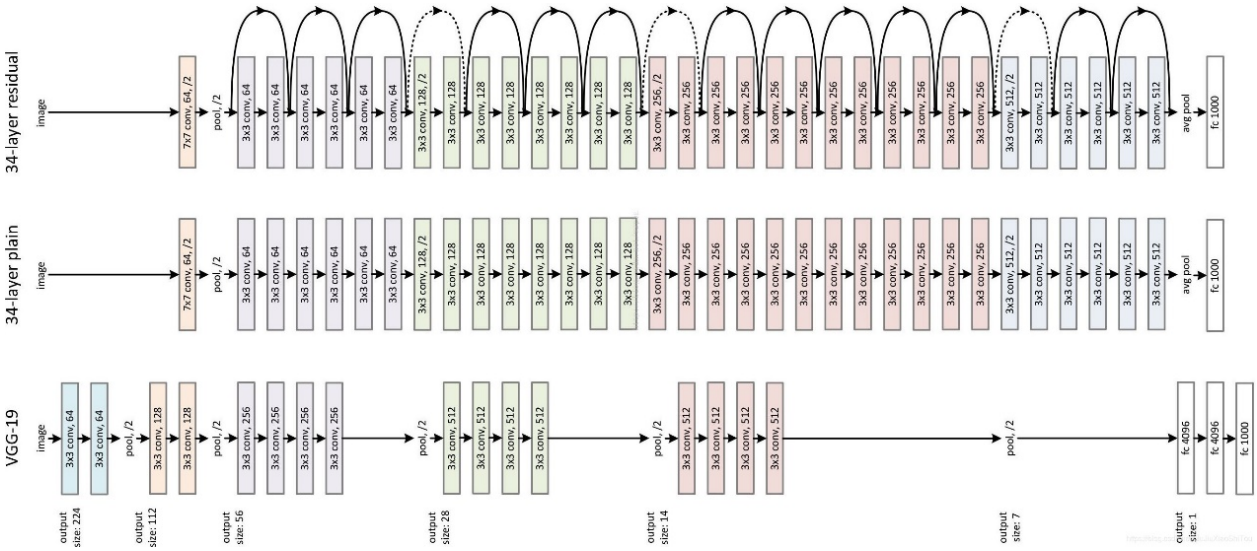

Figure 9. Resnet 50 Backbone model architecture [3]

2.3.2 Machine Learning Models and Training Datasets

ML models were developed varying the training dataset type and configurations per Table 1. The developed ML models were validated using three types of validation datasets as shown in Table 1. The validation dataset used for GMNN was only limited to validation data generated using GMNN method. Two different validation datasets were used to evaluate the efficiency of GMSN models. The validation datasets configuration for the developed models were selected based on the training dataset type. To validate the models trained with data generated from geometrical models, 2000 data points for each defect type was used. Validation of models trained with PD, actual inspections data of the fabricated defects were used. The number of validation data points used for models trained with PD was approximately 1200 data points for each defect type. Tables 2, 3, and 4 illustrate the model parameters used for GMNN, GMSN, and PD datasets respectively.

Table 2. Model parameters used for GMNN

Model Name	Training Dataset Type	Num. of Training Images per Defect Type	Pixel Size of the Training Image	Validation Data Type	Validation Images per Defect
LDSN32H1LX	GMNN	32	1 X Defect Length	GMNN	2000
LDSN32H1L1600			1 X 1600		
LDSN32H3LX			3 X Defect Length		
LDSN32H3L1600			3 X 1600		
LDSN1KH1LX		1K	1 X Defect Length		
LDSN1KH1L1600			1 X 1600		
LDSN1KH3LX			3 X Defect Length		
LDSN1KH3L1600			3 X 1600		

Table 3. Model parameters used for GMSN

Model Name	Training Dataset Type	Num. of Training Images per Defect Type	Pixel Size of the Training Image	Validation Data Type	Validation Images per Defect
SDSN32H1LX	GMSN	32	1 X Defect Length	GM - Simulated Noise & PM	2000
SDSN32H1L1600			1 X 1600		
SDSN32H3LX			3 X Defect Length		
SDSN32H3L1600			3 X 1600		
SDSN1KH1LX		1K	1 X Defect Length		
SDSN1KH1L1600			1 X 1600		
SDSN1KH3LX			3 X Defect Length		
SDSN1KH3L1600			3 X 1600		
SDSN10KH3NOAE*		10K	3 X Defect Length		
SDSN10KH3CSV**			3 X 1600		
SDSN10KH3LX			3 X Defect Length		
SDSN10KH3L1600			3 X 1600		

Notes:-

* A and E sections from the geometrical model was omitted.

** Training were annotated to highlight only the defect region of the image.

Table 4. Model parameters used for PD

Model Name	Training Dataset Type	Num. of Training Images per Defect Type	Pixel Size of the Training Image	Validation Data Type	Validation Images per Defect
PDSN32H3LX	PD	32	3 X Defect Length	GMNN GMSN PD	2000 1200
PDSN1KH1LX		1K	3 X Defect Length		
PDSN10KH3LX		10K	3 X Defect Length		

3. RESULTS AND DISCUSSION

ML models discussed in section 2.3.2 were validated using multiple datasets. The efficiency of the ML models were evaluated based on the classification accuracy. Number of correct classification for each defect type out of the validation data points was used to calculate the classification accuracy for each defect type. The overall model accuracy was calculated by averaging the accuracy percentages of all three defect types.

3.1.1 Defect Detection Accuracy Summary of Geometrical Model – No Noise (GMNN)

Figure 10 illustrates the defect detection accuracy of ML models trained with GMNN. The goal of using the GMNN dataset is to evaluate the efficiency of the model architecture to progress into training datasets with more realistic data. Overall, the GMNN models showed higher AFP defect classification accuracy for gap defects. For selected models, the detection accuracy of overlap defect was higher when lower number of training data points were used. The missing tow defects were the least accurately detected out of all the models trained with GMNN datasets. The reason for the low accuracy of detecting missing tow is because of the similarities seen between the gap and missing tow geometrical models. The only varying parameter in the gaps and missing tow geometrical models is segment c per Figure 3. This makes the two defect models geometrically identical in some instances. Overall, the use a single model did not perform to a satisfactory level to detect all three types of defects.

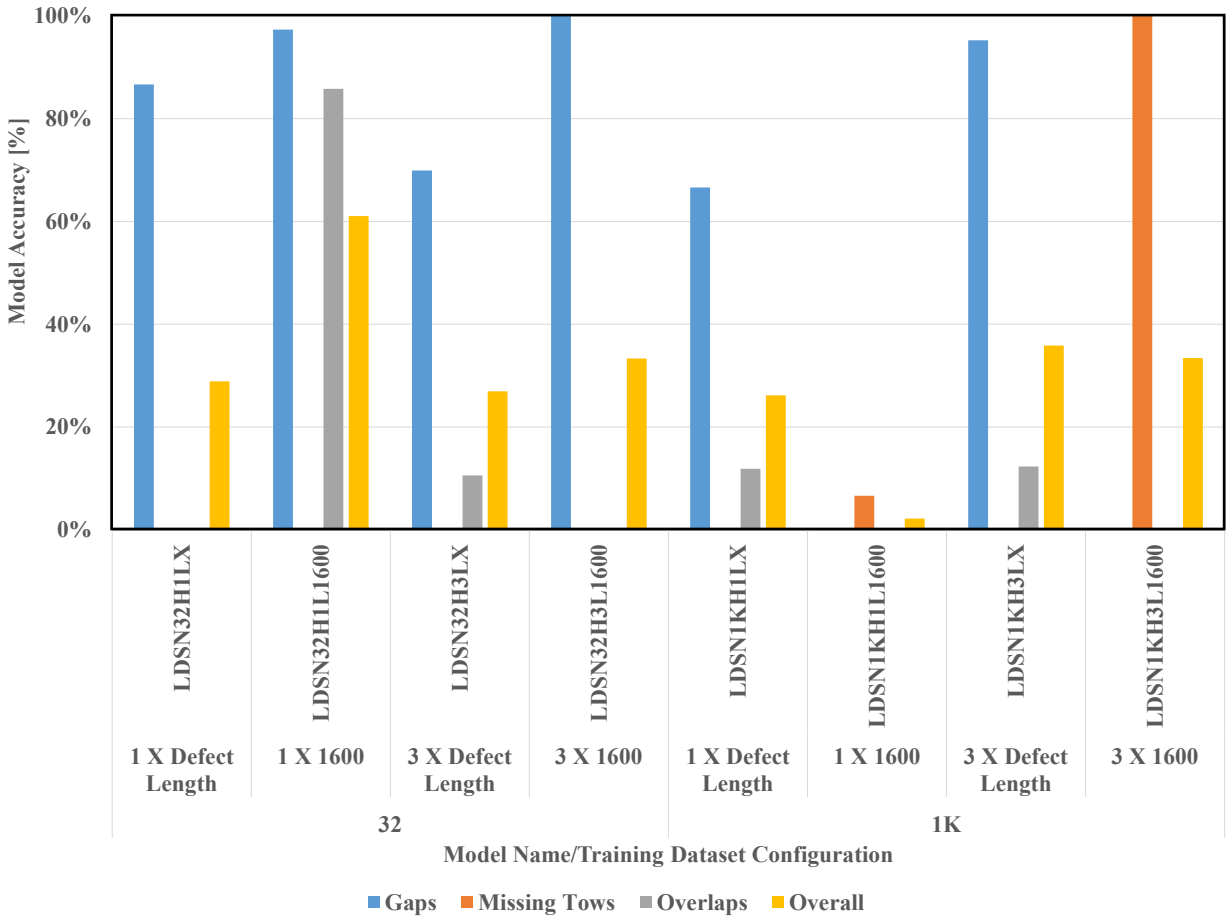

Figure 10. Defect detection accuracy summary of GMNN.

3.1.2 Defect Detection Accuracy Summary of Geometrical Model – Simulated Noise (GMSN)

Figure 11 illustrates the defect detection accuracy summary of models trained with GMSN with a range of different training datasets. Unlike the GMNN models, a single model was able to satisfactorily detect all three different types of defects with an accuracy of over 78%, yielding an overall model accuracy of 83%. The models trained with datasets with simulated noise, representing the surface roughness and surface morphology, showed a decrease in the effectiveness of the accuracy compared to models trained without simulated noise data. However, when larger training images and the number of training images per defect type was increased to 10K, a significant increase in the performance of the ML models was observed.

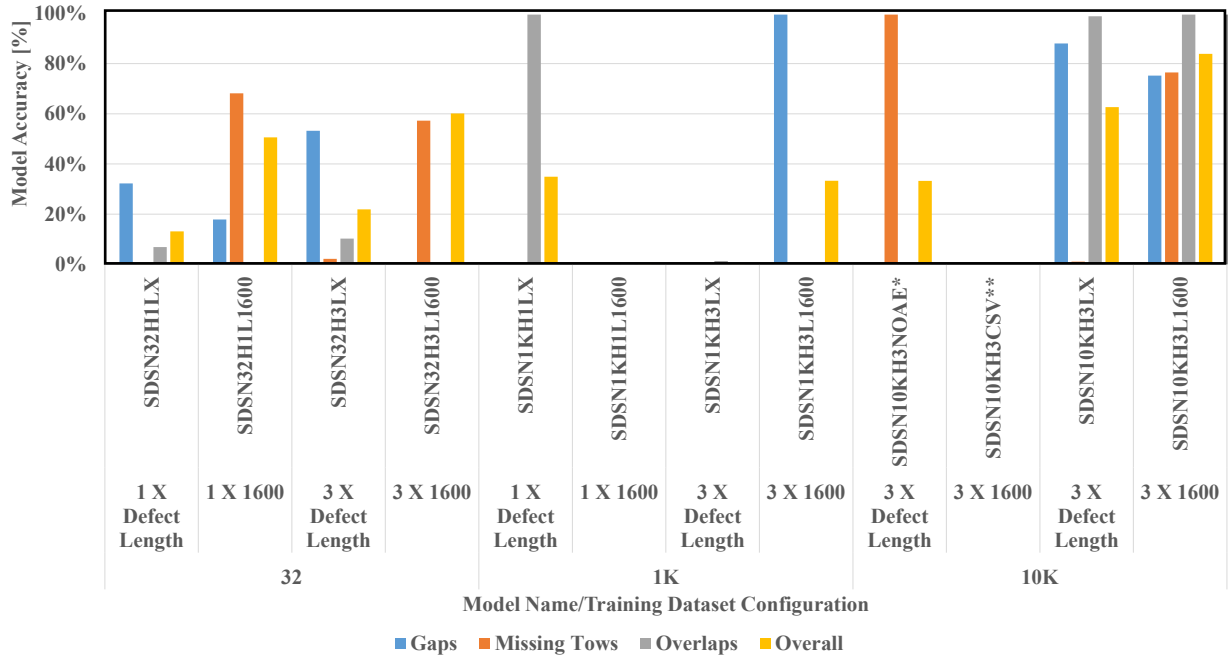

Figure 11. Defect detection accuracy summary of GMSN.

Figure 12 illustrates the model accuracy summary of ML models trained with GMSN and validated with PD. PD data was acquired from the profilometer and approximately 1200 data points for each defect type was acquired from the manufactured defects. The overall accuracy of the models showed the highest classification accuracy following the same trend as GMSM models trained with GMSM training data. With the data replicating more realistic scenarios, increase in the number of training datasets and the training image size improved the ML model classification accuracy. Overall trend of the models validated with PD showed a higher accuracy of classifying overlap AFP defects. The defect type with the minimum efficiency was gaps for validations completed with PD.

Based on the results from the GMNN and GMSN model validations, datasets were selected to train models with PD. The models performed over a selected percent accuracy was selected and trained with data generated from actual profilometer captured using the manufactured defects.

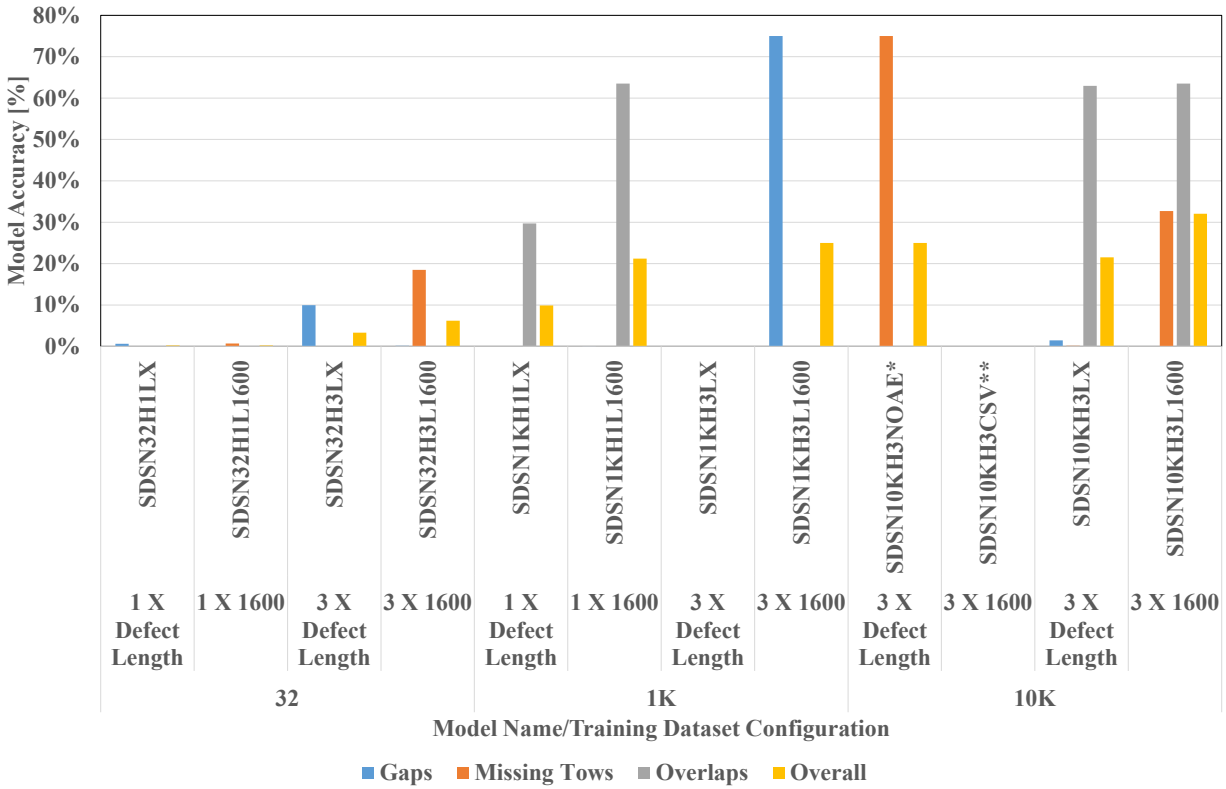

Figure 12. Defect detection accuracy summary of GMSN validated with PD.

3.1.3 Defect Detection Accuracy Summary of Geometrical Model – Profilometer Data (PD)

Figure 13 illustrates the ML model accuracy of the PD models validated against the GMNN dataset. Overall, all the models performed below satisfactory level. This is primarily due to the significant differences between the training dataset used to develop the model and validation dataset.

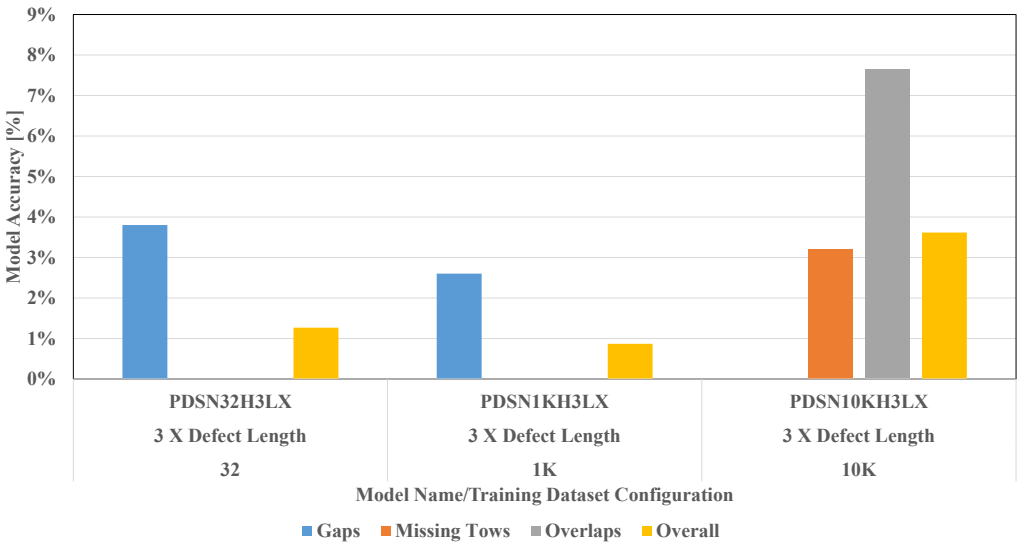

Figure 13. Defect detection accuracy summary of PD validated against GMNN.

Figure 14 illustrates the accuracy of the ML trained with PD validated against GMSN dataset. Compared to the previous validation performed on the GMNN dataset, the PD ML models performed better on the GMSN validation dataset. The GMSN validation data has a similar noise pattern of the noise level observed in the actual PD.

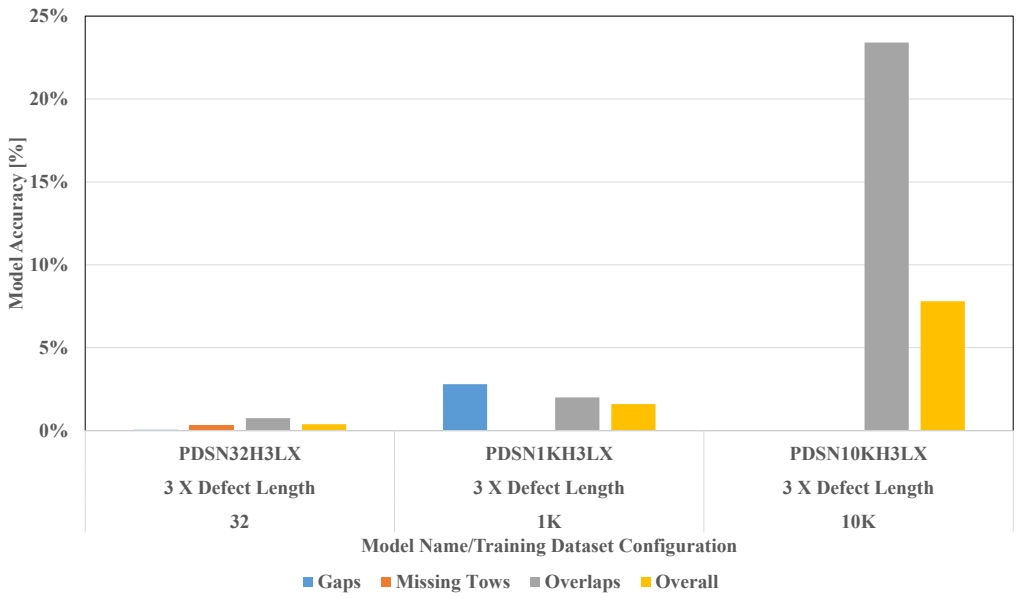

Figure 14. Defect detection accuracy summary of PD validated against GMSN.

Figure 15 illustrates the validation of the ML model trained with PD and validated against PD recorded during inspection of the fabricated defects. Overall, a significant increase in the accuracy was observed. However, all models performed poorly on classification of gap AFP defects. This could be due to the similarities seen in the geometrical models of gaps and missing tows.

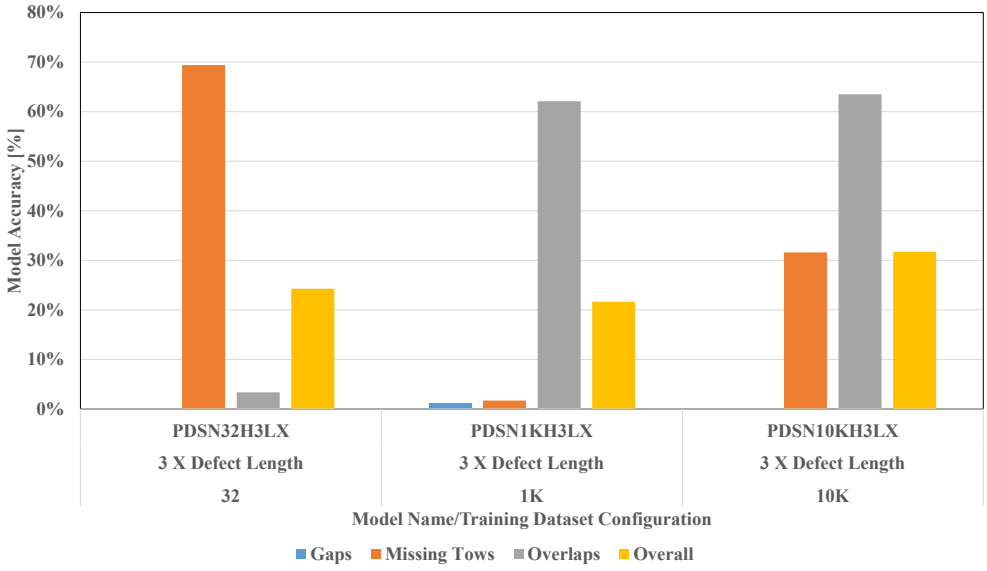

Figure 15. Defect detection accuracy summary of PD validated with PD.

4. CONCLUSIONS

Efficient and accurate in-process inspection systems are required to decrease the downtime of the AFP robots due to manual labor intensive inspections performed during manufacturing. With the advances in the sensor technologies, accurate and high-resolution data can be obtained during manufacturing process in order to support in-process inspections. Lack of efficient techniques to analyze large amount of inspection data require the use of a big data analytics. As a solution to big data analytics, ML models can be utilized efficiently. ML algorithms developed with sufficient amount of training data provide high confidence models used for detection and classification of defects. The amount of realistic training data captured in the production process may not be sufficient to develop efficient ML models. Therefore, training datasets are developed with the limited available realistic data to address the lack of available datasets for training ML models. The machine learning models trained through data generated using geometrical models showed favorable results for classification and detection of defects. The factors affecting the ML models proved to be the training image size and the number of images used in the training process. This can be effectively handled by creating more training data based on the geometrical models. The accuracy of the geometrical models can be further increased by incorporating physical characteristics of materials such as surface morphology and surface roughness. This technique can be expanded to other inspection methodologies such as optical and thermal inspections.

5. ACKNOWLEDGEMENTS

This research was funded by Air Force Research Laboratory (AFRL) under Modelling for Affordable, Sustainable Composites (MASC). Authors would like to thank Dr. David Mollenhauer for the support and technical guidance. The authors would also like to acknowledge and thank Aaron Jones for ML model training and Laura Sanchez Paredes for the training dataset development. Facts and opinions are solely the personal statements of the authors and do not necessarily represent the views of the sponsoring agency.

6. REFERENCES

[1] C. P. C. P. Tom Cooper. John Smiley, Global Fleet & MRO Market Forecast Commentary, Oliver Wyman, 2018.

[2] X. Z. S. R. J. S. Kaiming He, "Deep Residual Learning for Image Recognition," Microsoft Research, 2015.

[3] D. A. D. E. C. S. S. R. ,. C.-Y. F. A. C. B. Wei Liu, "SSD: Single Shot MultiBox Detector," UNC Chapel Hill 2, 2016.